

# Cellular and molecular features of lipoma tissue: comparison with normal adipose tissue

H. Suga, H. Eto, K. Inoue, N. Aoi, H. Kato, J. Araki, T. Higashino and K. Yoshimura

Department of Plastic Surgery, University of Tokyo Graduate School of Medicine, 7-3-1 Hongo, Bunkyo-Ku, Tokyo 113-8655, Japan

## Summary

### Correspondence

Kotaro Yoshimura.

E-mail: yoshimura-pla@h.u-tokyo.ac.jp

### Accepted for publication

20 April 2009

### Key words

adipogenesis, adipose progenitor cell, CD34, lipoma, obesity

### Conflicts of interest

None declared.

DOI 10.1111/j.1365-2133.2009.09272.x

**Background** Involvement of adipose-derived stem/progenitor/stromal cells (ASCs) in the development of lipomas has been suggested, but the pathogenesis and pathophysiology of this tumour remain unclear.

**Objectives** To analyse cellular and transcriptional characteristics of lipoma tissue compared with normal adipose tissue, further to delineate differentiating features.

**Methods** For lipoma or normal adipose tissues, we used a new whole-mount staining enabling three-dimensional imaging of nonfixed and nonfrozen adipose tissue. Immunohistochemistry and real-time polymerase chain reaction for obesity-related genes were performed as well as comparative assay of the proliferative and adipogenic capacity of ASCs.

**Results** A large number of small adipocytes surrounded by CD34+/ $\alpha$ actin- ASCs and increased numbers of Ki67+/CD34+ ASCs indicated enhanced adipogenesis in lipoma compared with normal adipose tissue. In contrast, cellular apoptosis was not enhanced in lipoma, suggesting that the enlargement of lipoma tissue may be due to a positive balance of adipocyte turnover (accelerated adipogenesis combined with nonenhanced apoptosis). Leptin mRNA was upregulated in lipoma, while adiponectin, tumour necrosis factor- $\alpha$  and glucose transporter 1 mRNA were downregulated and there were no apparent changes in hypoxia-inducible factor 1 $\alpha$ , peroxisome proliferator-activated receptor- $\gamma$  and plasminogen activator inhibitor-1. These results suggested dysfunction of lipoma adipocytes similar to that in obesity, but indicated that lipoma tissue lacked several obesity-related phenomena such as ischaemia (hypoxia), macrophage infiltration, inflammatory reactions and enhanced glycolysis. ASCs from lipoma and normal adipose tissue showed similar proliferative and adipogenic capacity.

**Conclusions** Our findings revealed that lipoma tissue shows a positive balance of adipocyte turnover involving proliferating ASCs and several transcriptional differences from adipose tissue enlargement in obesity.

Lipoma is a common benign neoplasm, which frequently arises in the subcutaneous tissues, is most commonly located in the trunk and proximal limbs,<sup>1</sup> and is demarcated from surrounding adipose tissue by a thin fibrous capsule. While lipomas are usually treated when small in size, they can grow larger than 10 cm and can weigh over 1 kg.<sup>2</sup> Although there are reports in the literature of proliferative activity<sup>3</sup> and chromosomal aberrations<sup>4</sup> of lipoma adipocytes, details of the cellular and molecular phenomena underlying the pathogenesis of this tumour remain unclear.

Adipocyte progenitor cells are found in normal adipose tissue;<sup>5,6</sup> the turnover rate of normal adipocytes is very slow.<sup>7</sup> Adipose progenitor cells have been shown to have the capacity

to differentiate into multiple lineages<sup>8,9</sup> and are referred to as adipose-derived stem/progenitor/stromal cells (ASCs).<sup>8</sup> Human ASCs have been determined to be CD34+ *in vitro*<sup>10</sup> and *in vivo*,<sup>11</sup> although they tend to lose CD34 expression with culture time. Spindle cell lipoma is also reported to be CD34+;<sup>12,13</sup> this type of lipoma consists of an intricate mixture of adipocytes and uniform spindle cells.<sup>14,15</sup>

Although ASCs can be isolated from human lipoma tissue,<sup>16</sup> detailed analysis of lipoma tissue at the cellular and molecular levels has rarely been performed. Conventional histological analysis of adipose tissue with frozen or paraffin-embedded sections has limitations that prevent accurate, detailed examination: freezing or fixation easily disrupts fragile adipocytes

and surrounding structures, and sectioning of the tissue leads to leakage of lipid contained in adipocytes; these artifactual alterations deform the original structure of adipose tissue. In this study, we employed a whole-mount immunohistological method that enables three-dimensional visualization of living adipose tissue stained with triple fluorescence.<sup>17,18</sup> In addition, we analysed cellular and transcriptional characteristics of lipoma tissue and normal adipose tissue, which may provide new insights into the pathogenesis and pathophysiology of lipomas.

## Materials and methods

### Clinical data

Intact adipose tissue alone ( $n = 2$ ), lipoma tissue alone ( $n = 2$ ), or both ( $n = 3$ ) were obtained from seven nonobese patients (mean  $\pm$  SEM body mass index  $22.3 \pm 1.1 \text{ kg m}^{-2}$ ) who underwent plastic surgery or tumour resection. The patients were four men and three women aged  $47.0 \pm 5.7$  years (mean  $\pm$  SEM) (Table 1). Informed consent was obtained from each patient using a protocol approved by the institutional review board.

### Whole-mount staining

Visualization of nonfixed and nonsectioned adipose tissues was performed using a whole-mount staining as previously described.<sup>17,18</sup> Briefly, adipose tissue samples were minced into 3-mm pieces and incubated with the following reagents for 30 min at 37 °C: BODIPY 558/568 ( $5 \mu\text{g mL}^{-1}$ ; Molecular Probes, Eugene, OR, U.S.A.) was used to stain adipocytes, Alexa Fluor 488-conjugated isolectin GS-IB<sub>4</sub> (lectin) ( $5 \mu\text{g mL}^{-1}$ ; Molecular Probes) to stain endothelial cells, and Hoechst 33342 ( $5 \mu\text{g mL}^{-1}$ ; Dojindo, Kumamoto, Japan) to stain nuclei. For CD34 immunostaining, the tissue sample was fixed in 4% paraformaldehyde for 30 min and incubated with a primary antibody (mouse antihuman CD34) (clone QBEnd 10, dilution 1 : 500; Dako, Glostrup, Denmark) overnight at

Table 1 Clinical data of patients and respective symbols in the figures

Symbol	Patient	Age (years)/sex	BMI ( $\text{kg m}^{-2}$ )	Adipocyte source	Site
●	1	58/M	18.8	Lipoma and normal	Back
▲	2	40/M	25.8	Lipoma and normal	Abdomen
■	3	73/F	18.5	Lipoma and normal	Arm
×	4	31/F	20.5	Lipoma	Arm
○	5	53/M	23.6	Lipoma	Forehead
△	6	40/M	24.7	Normal	Abdomen
□	7	34/F	24.3	Normal	Abdomen

BMI, body mass index.

4 °C. The sample was then washed and incubated with a secondary antibody (Alexa Fluor 568-conjugated goat antimouse IgG) (dilution 1 : 200; Molecular Probes), together with lectin and Hoechst 33342. Each stained sample was directly observed with a confocal microscope system (Leica TCS SP2; Leica Microsystems, Wetzlar, Germany). Thirty serial images were obtained at 1- $\mu\text{m}$  intervals and the acquired images were processed to produce a surface-rendered 30- $\mu\text{m}$  thick three-dimensional image.

### Immunohistochemistry

Harvested adipose tissues were zinc-fixed (Zinc Fixative; BD Biosciences, San Diego, CA, U.S.A.) and paraffin-embedded. We prepared 6- $\mu\text{m}$  thick sections and performed immunostaining using the following primary antibodies: mouse antihuman CD34 (clone QBEnd 10, dilution 1 : 500; Dako) and rabbit antihuman Ki67 (clone SP6, dilution 1 : 200; Thermo Fisher Scientific, Fremont, CA, U.S.A.) or mouse antihuman CD68 (clone KP1, dilution 1 : 100; Dako). Isotypic antibody was used as a negative control for each staining. For visualization with diaminobenzidine, peroxidase-conjugated secondary antibodies appropriate for each primary antibody (Nichirei Biosciences, Tokyo, Japan) were used. Nuclei were counterstained with haematoxylin. For double-fluorescence staining, Alexa Fluor 488-conjugated goat antimouse IgG and Alexa Fluor 568-conjugated goat antirabbit IgG (both dilution 1 : 200; Molecular Probes) were used as secondary antibodies. Nuclei were stained with 4',6-diamidino-2-phenylindole. To detect apoptosis, terminal deoxynucleotidyl transferase-mediated deoxyuridine triphosphate nick end-labelling (TUNEL) staining was performed using an in situ Cell Death detection kit (Roche Diagnostics, Mannheim, Germany).

### Quantitative real-time polymerase chain reaction

Total RNA was isolated from the samples using an RNeasy Mini Kit (Quiagen, Hilden, Germany), followed by reverse transcription. Real-time polymerase chain reaction (PCR) was performed with the ABI 7700 sequence detection system and a SYBR Green PCR master mix (both from Applied Biosystems, Foster City, CA, U.S.A.); the primer sequences used are shown in Table 2. Expression levels were calculated by the comparative  $C_T$  method using glyceraldehyde-3-phosphate dehydrogenase as an endogenous reference gene.

### Stromal cell isolation and culture

Adipose tissue samples were minced into 2–3-mm pieces and digested on a shaker in phosphate-buffered saline containing 0.075% collagenase (Wako Chemicals, Osaka, Japan) for 30 min at 37 °C. Mature adipocytes and connective tissue were separated from pellets by centrifugation (800 g, 10 min). The stromal vascular fraction cells containing ASCs were resuspended, filtered through 100- $\mu\text{m}$  mesh, plated at a density of  $2 \times 10^5$  nucleated cells/60-mm dish, and cultured

**Table 2** Primer sequences used in real-time polymerase chain reaction

Gene	Primer sequence (5'-3')
Leptin	Forward: TGGTGGGTTCTTTGGAAGGAGTGA Reverse: GGATTTGAAGCAAAGCACCAGCCT
PPAR $\gamma$	Forward: CTGTTTCCAAGCTGTCCAGAAA Reverse: AAGAAGGGAATGTTGGCAGTGGC
Adiponectin	Forward: ACCATGAGCAATTCTCCTGCCTCA Reverse: TGATGGCTCATGCCTGTAATCCCA
HIF1 $\alpha$	Forward: TTGGCAGCAACGACACAGAACTG Reverse: TTGAGTGCAAGGTCAGCACTACTT
TNF- $\alpha$	Forward: AGGACGAACATCCAACCTTCCCAA Reverse: TTTGAGCCAGAAGAGGTTGAGGGT
PAI-1	Forward: TCTGCCCTACCAACATTCTGAGT Reverse: ACATGTCGGTCATTCCAGGTCT
GLUT1	Forward: ATCGTGGCCATCTTTGGCTTTGTG Reverse: CTGGAAGCATGCCCACAATGAA
GAPDH	Forward: CATGTTTCGTCATGGGTGTGAACCA Reverse: AGTGATGGCATGGACTGTGGTCAT

PPAR $\gamma$ , peroxisome proliferator-activated receptor- $\gamma$ ; HIF1 $\alpha$ , hypoxia-inducible factor 1 $\alpha$ ; TNF- $\alpha$ , tumour necrosis factor- $\alpha$ ; PAI-1, plasminogen activator inhibitor-1; GLUT1, glucose transporter 1; GAPDH, glyceraldehyde-3-phosphate dehydrogenase.

at 37 °C in an atmosphere of 5% CO<sub>2</sub> in humid air. Primary cells, defined as 'passage 0', were cultured with Dulbecco's modified Eagle's medium (DMEM) (Nissui Pharmaceutical, Tokyo, Japan) containing 10% fetal bovine serum (FBS) and cells other than ASCs (such as endothelial cells and leucocytes) were almost excluded by the adherent culture for 1 week. The medium was replaced every 3 days and the cells were sub-cultured every week by trypsinization.

### Adipogenic differentiation assay

The stromal vascular fraction cells at passage 1, most of which are composed of ASCs, were incubated for 21 days in DMEM containing 10% FBS, 0.5 mmol L<sup>-1</sup> isobutyl-methyl-xanthine, 1  $\mu$ mol L<sup>-1</sup> dexamethasone, 10  $\mu$ mol L<sup>-1</sup> insulin and 200  $\mu$ mol L<sup>-1</sup> indomethacin. Adipogenic differentiation was visualized with Oil Red O staining. For quantitative analysis of lipid droplets, Nile Red fluorescence (AdipoRed; Cambrex, Walkersville, MD, U.S.A.) was measured with excitation at 485 nm and emission at 535 nm.

### Statistical analysis

Results were expressed as mean  $\pm$  SEM. Comparisons between two groups were performed with Welch's *t*-test. *P* < 0.05 was considered significant.

## Results

### Whole-mount histology of living tissues

Whole-mount histology showed nonruptured adipocytes with capillaries located alongside the adipocytes, forming a

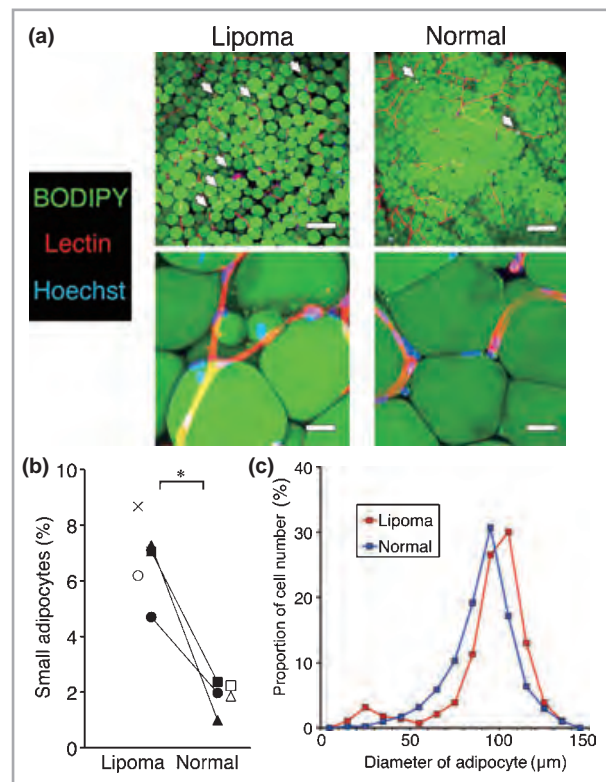


**Fig 1.** Morphological assessment of adipocytes. (a) Whole-mount staining of lipoma and normal adipose tissue. Original structures of adipocytes and adipose tissue are preserved and capillary networks running alongside adipocytes are well visualized. Scale bars = 200  $\mu$ m (upper panels) or 25  $\mu$ m (lower panels). (b) Numerical proportion of small adipocytes (< 50  $\mu$ m). Small adipocyte number was significantly higher in lipoma tissue (\**P* < 0.05). Each symbol corresponds to a sample donor shown in Table 1. Bars show mean  $\pm$  SEM. (c) A representative histogram of adipocyte diameter. A peak of small adipocytes (20–30  $\mu$ m) was found in lipoma adipocytes, although the main populations are similar in size between lipoma and normal adipose tissue.

well-organized network in both lipoma and normal adipose tissue (Fig. 1a; adipocytes in green and capillaries in red). Capillaries and vessels were abundant in both tissues, and no apparent difference in vascular density was observed (Fig. 1a). Small adipocytes (< 50  $\mu$ m in diameter) were detected in both tissues; the proportion of these small adipocytes was significantly greater in lipoma tissue (6.78  $\pm$  0.66%) vs. normal adipose tissue (1.88  $\pm$  0.24%) (Fig. 1a,b). The mode of adipocyte diameter was comparable between lipoma and normal tissue (approximately 90–110  $\mu$ m), but adipocyte size in lipoma tissue showed a bimodal distribution with a second peak at 20–30  $\mu$ m (Fig. 1c). These results suggest enhanced adipogenesis in lipoma tissue.

Combination staining with CD34 and lectin on whole-mount tissue showed CD34+/lectin- ASCs present alongside capillaries and in interstitial spaces in both lipoma and normal adipose tissue. Furthermore, it was frequently observed that CD34+ ASCs aggregated around small adipocytes in lipoma

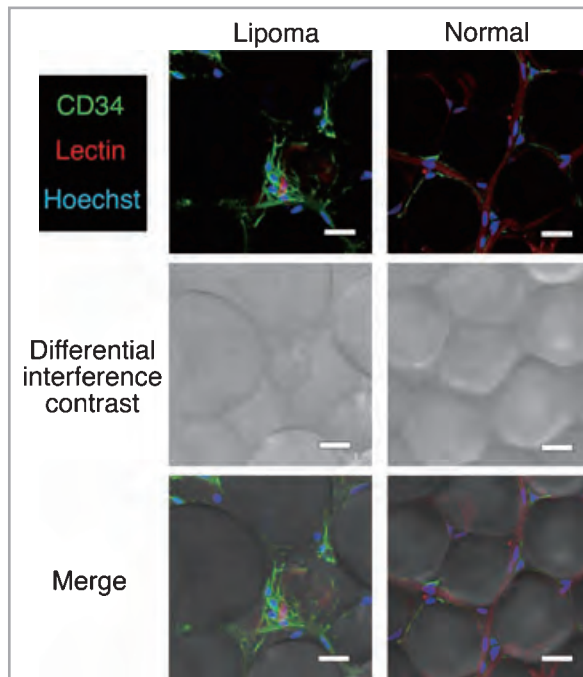


Fig 2. Whole-mount immunohistology of lipoma and normal adipose tissue. CD34<sup>+</sup> cells aggregated around a small adipocyte in lipoma tissue, which is suggested to be a feature indicating adipogenesis. Scale bars = 25  $\mu$ m.

tissue, forming a cell cluster suggestive of adipocyte neogenesis (Fig. 2).

### Histology of fixed sections

Using fixed tissue sections, we examined cell proliferation, apoptosis and macrophage infiltration. Immunohistochemical staining for Ki67 indicated that the proportion of Ki67<sup>+</sup> proliferating cells was significantly higher in lipoma tissue ( $6.90 \pm 1.12\%$ ) compared with normal adipose tissue ( $2.41 \pm 0.61\%$ ) (Fig. 3a,b). Double-fluorescence immunostaining for Ki67 and CD34 revealed that most Ki67<sup>+</sup> proliferating cells in lipoma were also positive for CD34 (Fig. 3c). These results suggest that ASCs are the primary proliferating cell population and contribute to enhanced adipogenesis in lipoma.

TUNEL staining indicated that there were no differences in apoptotic cell number between lipoma and normal adipose tissue (Fig. 4a,b). Immunohistochemical staining for CD68 showed that CD68<sup>+</sup> macrophages were rare in both lipoma and normal adipose tissue; crown-like structures, a feature of adipocyte phagocytosis by infiltrating macrophages frequently seen in obese adipose tissue,<sup>19–21</sup> was not observed (data not shown).

### Assays for expression of obesity-related genes

Expression of selected obesity-related genes was examined with real-time PCR (Fig. 5). Leptin expression was higher and adiponectin expression was lower in lipoma tissue compared with

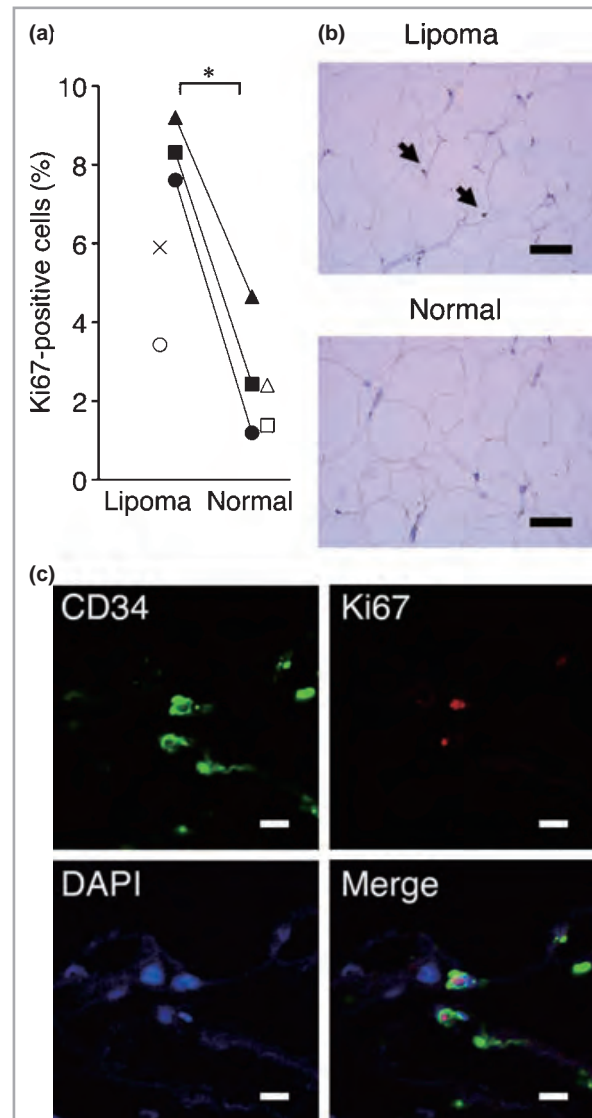
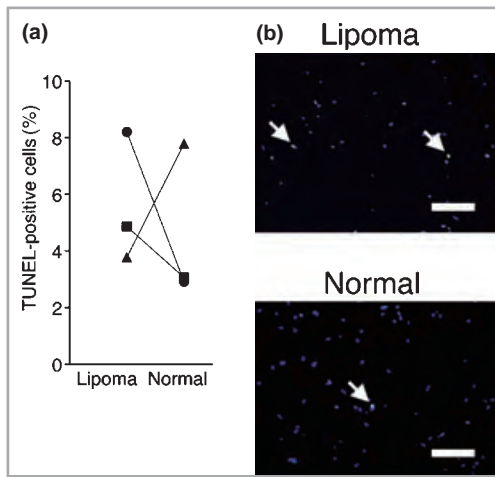


Fig 3. Proliferating cells in lipoma and normal adipose tissue. (a) Numerical proportion of Ki67<sup>+</sup> proliferating cells. Proliferating cell number was significantly higher in lipoma ( $*P < 0.05$ ). Each symbol corresponds to a sample donor shown in Table 1. Bars show mean  $\pm$  SEM. (b) Immunostained images for Ki67. Black arrows indicate Ki67<sup>+</sup> cells located between adipocytes. Scale bars = 50  $\mu$ m. (c) Double-fluorescence immunostained images for Ki67 (red) and CD34 (green) in lipoma tissue. Nuclei were stained with 4',6-diamidino-2-phenylindole (blue). Most Ki67<sup>+</sup> proliferating cells are also positive for CD34, suggesting that they are adipose-derived stem/progenitor/stromal cells. Scale bars = 10  $\mu$ m.

normal adipose tissue in all three patients from whom both tissues were harvested; this expression pattern is a characteristic finding in obesity.<sup>22,23</sup> Tumour necrosis factor (TNF)- $\alpha$ , hypoxia-inducible factor 1 $\alpha$  (HIF1 $\alpha$ ), plasminogen activator inhibitor-1 (PAI-1) and glucose transporter 1 (GLUT1) are known to be upregulated in obesity.<sup>22,23</sup> However, in our samples no apparent difference in expression of HIF1 $\alpha$  and PAI-1 was detected between lipoma and normal adipose tissue, while



**Fig 4.** Apoptosis in lipoma and normal adipose tissue. (a) Numerical proportion of apoptotic cells. There were no differences between lipoma and normal adipose tissue. Each symbol corresponds to a sample donor shown in Table 1. Bars show mean  $\pm$  SEM. (b) Terminal deoxynucleotidyl transferase-mediated deoxyuridine triphosphate nick end-labelling (TUNEL) staining (green) of adipose tissue. Nuclei were stained with 4',6-diamidino-2-phenylindole (DAPI) (blue). White arrows indicate TUNEL+/DAPI+ nuclei. Scale bars = 100  $\mu$ m.

expression of TNF- $\alpha$  and GLUT1 were downregulated in lipoma tissue of all three patients. Expression of peroxisome proliferator-activated receptor- $\gamma$  (PPAR $\gamma$ ) in lipoma tissue was not distinctly different from that in normal adipose tissue.

**Assays for adipose progenitor cell functions**

ASCs were isolated and cultured from lipoma and normal adipose tissue. Adipogenesis was easily induced in ASCs from both tissues, and there was no difference in the capacity for adipogenic differentiation (Fig. 6a,b). Long-term adherent culture showed that both cell populations possess similar expansion potentials at least up to passage 10 (Fig. 6c). There were no morphological differences between the cells from lipoma and normal adipose tissue after long-term culture (Fig. 6d). Thus, we did not detect any functional differences between ASCs from lipoma and normal adipose tissue in *in vitro* assessments, although they apparently behave differently *in vivo*.

**Discussion**

Our findings indicate that ASCs in lipoma tissue are actively proliferating and contribute to enhanced adipogenesis. A cell

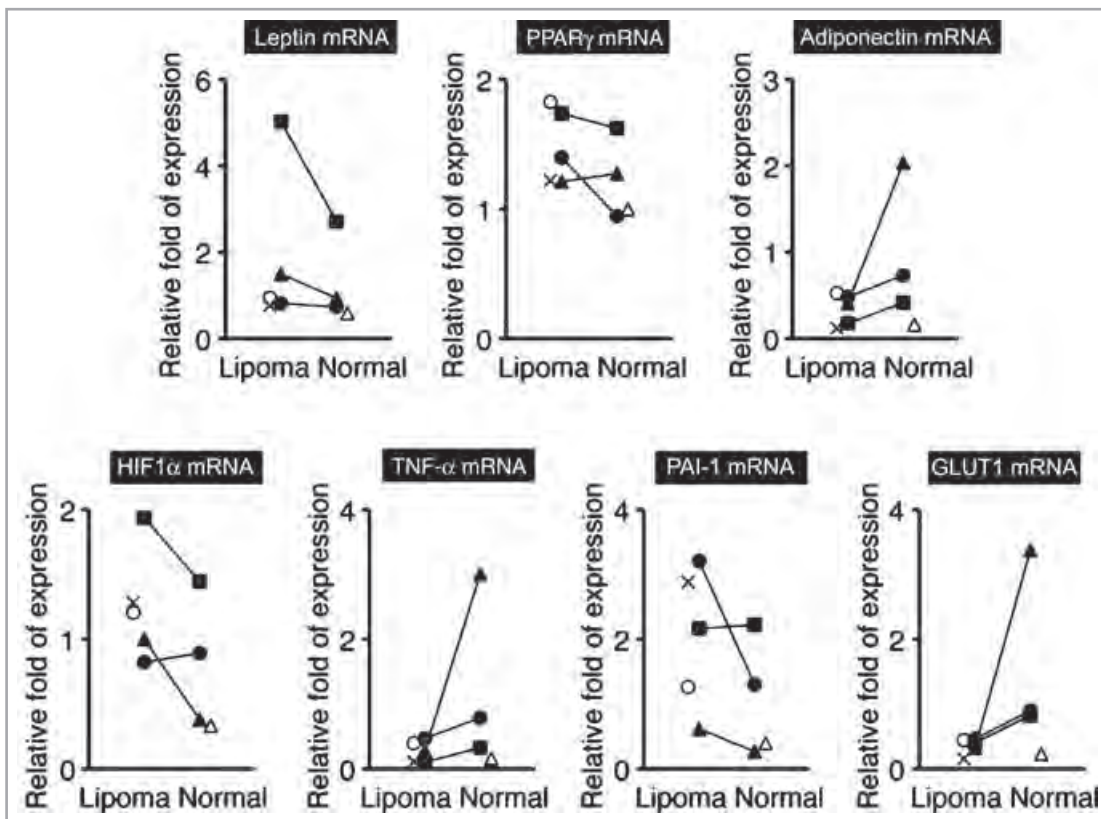


**Fig 5.** Transcriptional profiles of lipoma and normal adipose tissue. PPAR $\gamma$ , peroxisome proliferator-activated receptor- $\gamma$ ; HIF1 $\alpha$ , hypoxia-inducible factor 1 $\alpha$ ; TNF- $\alpha$ , tumour necrosis factor- $\alpha$ ; PAI-1, plasminogen activator inhibitor-1; GLUT1, glucose transporter 1. In lipoma, upregulation of leptin mRNA, and downregulation of adiponectin, TNF- $\alpha$  and GLUT1 mRNA were observed. Each symbol corresponds to a sample donor shown in Table 1. Bars show mean  $\pm$  SEM.

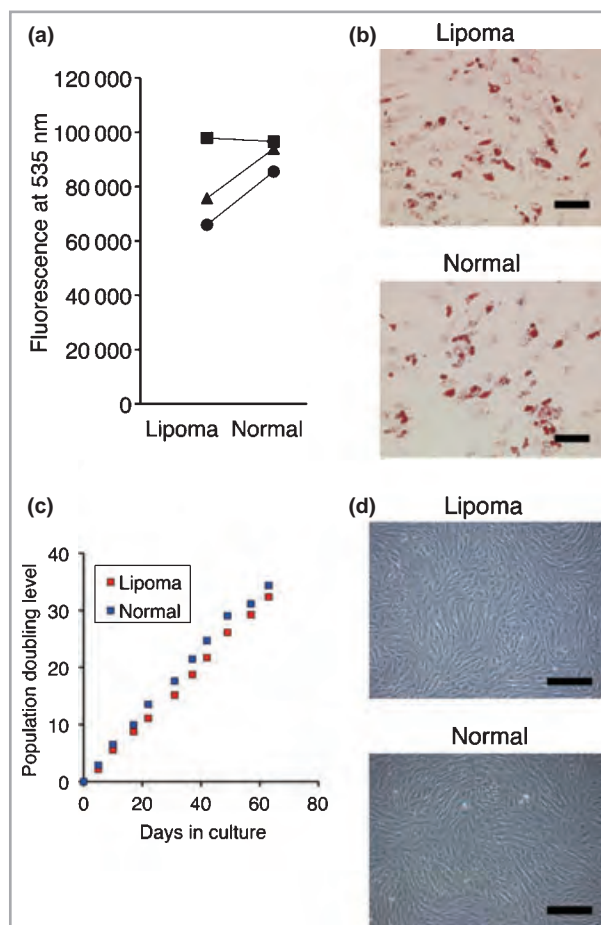


**Fig 6.** Adipogenic differentiation and proliferation capacities of adipose-derived stem/progenitor/stromal cells (ASCs) isolated from lipoma and normal adipose tissue. (a) Quantitative measurement of Nile Red fluorescence after adipogenic differentiation. There were no differences in lipid content between adipogenic-differentiated cells from lipoma and normal adipose tissue. Each symbol corresponds to a sample donor shown in Table 1. Bars show mean  $\pm$  SEM. (b) Oil Red O stained images after adipogenic differentiation. Scale bars = 100  $\mu$ m. (c) Population doubling level of cultured ASCs. There were no differences in expansion capacity between ASCs from lipoma and normal adipose tissue. (d) Light micrographs of cultured ASCs at passage 10. Scale bars = 400  $\mu$ m.

aggregation formed with a small adipocyte surrounded by CD34<sup>+</sup> ASCs seen in lipoma tissue is a characteristic finding suggesting adipogenesis, which was also seen in diabetic obese mice and is called an adipogenic/angiogenic cell cluster.<sup>17</sup> In these cell clusters, it is likely that ASCs are proliferating and supporting the small differentiating adipocytes.

Our results also showed that apoptotic adipocyte number is comparable in lipoma and normal adipose tissue, suggesting that the enlargement of lipoma tissue may be due to the positively preserved balance of adipocyte turnover (accelerated adipogenesis with nonenhanced apoptosis). A previous study demonstrated proliferation of cells alongside vessels in lipoma;<sup>3</sup> the proliferating cells seem to be ASCs, based on previous demonstration of a perivascular localization for

ASCs<sup>6,11,24</sup> as well as in this study. In spindle cell lipoma, an intricate mixture of adipocytes and uniform spindle cells,<sup>14,15</sup> which were strongly positive for CD34, were observed;<sup>12,13</sup> the CD34<sup>+</sup> ASCs may be expanding at a greater rate than that seen in normal adipogenesis. Our study showed no apparent differences in properties or functional status of ASCs derived from lipoma and normal adipose tissue *in vitro*, even though they behave differently *in vivo*. This finding suggests that increased activity of lipoma ASCs may be highly dependent on genetic or microenvironmental factors. PPAR $\gamma$  plays a central role in adipocyte differentiation<sup>6,25</sup> and activation of PPAR $\gamma$  signalling induces terminal differentiation of human liposarcoma cells.<sup>25–27</sup> PPAR $\gamma$  expression did not differ between lipoma and normal adipose tissue, suggesting involvement of other mechanisms in lipoma, such as injury-associated factors.<sup>28</sup>

It is of great interest that our lipoma tissues showed some features in common with and some distinct from obesity. Similar to obese adipocytes, lipoma-derived adipocytes showed upregulation of leptin and downregulation of adiponectin; this suggested impaired endocrine function of lipoma adipocytes. However, in contrast to obese adipocytes, lipoma adipocytes lacked macrophage infiltrations, upregulation of TNF- $\alpha$  and HIF1 $\alpha$ , and increased glycolysis (GLUT1 and PAI-1). Recent studies indicated that adipose tissue in obesity is hypoxic, and this hypoxia is a basis for the dysregulation of tissue function in obesity.<sup>22,23</sup> Hypoxia in obese adipose tissue induces HIF1 $\alpha$  upregulation, activates glycolytic processes, and induces adipocyte apoptosis/necrosis, which further recruits macrophages and enhances inflammatory reactions.<sup>19</sup> Infiltrated macrophages play a crucial role in the development of obesity-related insulin resistance<sup>21</sup> and upregulation of inflammatory cytokines such as TNF- $\alpha$ .<sup>20</sup> Our results showed that hypoxia-related genes, such as HIF1 $\alpha$ , GLUT1 and PAI-1, were not upregulated in lipoma samples, suggesting that normal oxygen pressure in lipoma tissue is preserved. Although adipogenesis is accelerated in lipoma, lipoma tissue escapes from hypoxia and does not show enhanced apoptosis, macrophage infiltration, or subsequent inflammatory changes. A potential explanation for this finding is that angiogenesis may be successfully increasing alongside adipogenesis, and this may be the reason for maintenance of oxygen pressure in lipoma. We previously reported a case of lipedema, in which increased adipogenesis and proliferating ASCs were observed in the tissue, similar to lipoma; however, lipedema tissue also showed hypoxia-associated features such as adipocyte death and macrophage recruitment.<sup>29</sup>

In conclusion, comparative analyses of lipoma and normal adipose tissue showed enhanced adipogenesis and nonenhanced adipocyte apoptosis in lipoma tissue, involvement of CD34<sup>+</sup>/lectin<sup>–</sup> ASCs in the adipogenesis/angiogenesis process, and adipocyte dysfunction such as upregulation of leptin and downregulation of adiponectin. We also found that lipoma tissue lacked several obesity-related phenomena such as ischaemia (hypoxia), macrophage infiltration, inflammatory reactions and enhanced glycolysis. Functional differences of

tissue progenitor cells were not detected, suggesting that the increased adipogenesis/angiogenesis may be dependent on microenvironmental factors of lipoma tissue, although further studies will be needed to elucidate detailed mechanisms underlying this phenomenon.

## Acknowledgments

We thank Ayako Kurata for her technical assistance. This work was supported by a grant from the Japanese Ministry of Education, Culture, Sports, Science, and Technology (contact grant number: B2-19390452).

## References

- Dalal KM, Antonescu CR, Singer S. Diagnosis and management of lipomatous tumors. *J Surg Oncol* 2008; **97**:298–313.
- Silistreli OK, Drumus EU, Ulusal BG *et al.* What should be the treatment modality in giant cutaneous lipomas? Review of the literature and report of 4 cases *Br J Plast Surg* 2005; **58**:394–8.
- Kolokol'chikova EG, Pal'tsyn AA, Shchegolev AI *et al.* Proliferative activity of adipocytes in adipose tissue tumors. *Bull Exp Biol Med* 2005; **140**:122–6.
- Willen H, Akerman M, Dal Cin P *et al.* Comparison of chromosomal patterns with clinical features in 165 lipomas: a report of the CHAMP study group. *Cancer Genet Cytogenet* 1998; **102**:46–9.
- Rodeheffer MS, Birsoy K, Friedman JM. Identification of white adipocyte progenitor cells in vivo. *Cell* 2008; **135**:240–9.
- Tang W, Zeve D, Suh JM *et al.* White fat progenitor cells reside in the adipose vasculature. *Science* 2008; **322**:583–6.
- Spalding KL, Arner E, Westermark PO *et al.* Dynamics of fat cell turnover in humans. *Nature* 2008; **453**:783–7.
- Gimble JM, Katz AJ, Bunnell BA. Adipose-derived stem cells for regenerative medicine. *Circ Res* 2007; **100**:1249–60.
- Zuk PA, Zhu M, Ashjian P *et al.* Human adipose tissue is a source of multipotent stem cells. *Mol Biol Cell* 2002; **13**:4279–95.
- Yoshimura K, Shigeura T, Matsumoto D *et al.* Characterization of freshly isolated and cultured cells derived from the fatty and fluid portions of liposuction aspirates. *J Cell Physiol* 2006; **208**:64–76.
- Traktuev DO, Merfeld-Clauss S, Li J *et al.* A population of multipotent CD34-positive adipose stromal cells share pericyte and mesenchymal surface markers, reside in a periendothelial location, and stabilize endothelial networks. *Circ Res* 2008; **102**:77–85.
- Suster S, Fisher C. Immunoreactivity for the human hematopoietic progenitor cell antigen (CD34) in lipomatous tumors. *Am J Surg Pathol* 1997; **21**:195–200.
- Templeton AF, Solomon AR Jr. Spindle cell lipoma is strongly CD34 positive. An immunohistochemical study. *J Cutan Pathol* 1996; **23**:546–50.
- Bolen JW, Thorning D. Spindle-cell lipoma. A clinical, light- and electron-microscopical study. *Am J Surg Pathol* 1981; **5**:435–41.
- Enzinger FM, Harvey DA. Spindle cell lipoma. *Cancer* 1975; **36**:1852–9.
- Lin TM, Chang HW, Wang KH *et al.* Isolation and identification of mesenchymal stem cells from human lipoma tissue. *Biochem Biophys Res Commun* 2007; **361**:883–9.
- Nishimura S, Manabe I, Nagasaki M *et al.* Adipogenesis in obesity requires close interplay between differentiating adipocytes, stromal cells, and blood vessels. *Diabetes* 2007; **56**:1517–26.
- Suga H, Eto H, Shigeura T *et al.* IFATS collection. Fibroblast growth factor-2-induced hepatocyte growth factor secretion by adipose-derived stromal cells inhibits postinjury fibrogenesis through a c-Jun N-terminal kinase-dependent mechanism. *Stem Cells* 2009; **27**:238–49.
- Cinti S, Mitchell G, Barbatelli G *et al.* Adipocyte death defines macrophage localization and function in adipose tissue of obese mice and humans. *J Lipid Res* 2005; **46**:2347–55.
- Weisberg SP, McCann D, Desai M *et al.* Obesity is associated with macrophage accumulation in adipose tissue. *J Clin Invest* 2003; **112**:1796–808.
- Xu H, Barnes GT, Yang Q *et al.* Chronic inflammation in fat plays a crucial role in the development of obesity-related insulin resistance. *J Clin Invest* 2003; **112**:1821–30.
- Hosogai N, Fukuhara A, Oshima K *et al.* Adipose tissue hypoxia in obesity and its impact on adipocytokine dysregulation. *Diabetes* 2007; **56**:901–6.
- Trayhurn P, Wang B, Wood IS. Hypoxia in adipose tissue: a basis for the dysregulation of tissue function in obesity? *Br J Nutr* 2008; **100**:227–35.
- Lin G, Garcia M, Ning H *et al.* Defining stem and progenitor cells within adipose tissue. *Stem Cells Dev* 2008; **17**:1053–63.
- Tontonoz P, Singer S, Forman BM *et al.* Terminal differentiation of human liposarcoma cells induced by ligands for peroxisome proliferator-activated receptor  $\gamma$  and the retinoid X receptor. *Proc Natl Acad Sci USA* 1997; **94**:237–41.
- Debrock G, Vanhentenrijk V, Sciot R *et al.* A phase II trial with rosiglitazone in liposarcoma patients. *Br J Cancer* 2003; **89**:1409–12.
- Demetri GD, Fliecher CD, Mueller E *et al.* Induction of solid tumor differentiation by the peroxisome proliferator-activated receptor- $\gamma$  ligand troglitazone in patients with liposarcoma. *Proc Natl Acad Sci USA* 1999; **96**:3951–6.
- Signorini M, Campiglio GL. Posttraumatic lipomas: where do they really come from? *Plast Reconstr Surg* 1998; **101**:699–705.
- Suga H, Araki J, Aoi N *et al.* Adipose tissue remodeling in lipedema: adipocyte death and concurrent regeneration. *J Cutan Pathol* 2009 [Epub ahead of print].